The role of autophagy in the death of L1210 leukemia cells initiated by the new antitumor agents, XK469 and SH80

David Kessel,[1] John J. Reiners, Jr.,[2] Stuart T. Hazeldine,[3] Lisa Polin,[3] and Jerome P. Horwitz[3]

[1]Department of Pharmacology, Wayne State University School of Medicine; [2]Institute of Environmental Health Sciences, Wayne State University; and [3]Department of Internal Medicine, Division of Hematology and Oncology, Wayne State University School of Medicine and Barbara Ann Karmanos Cancer Institute, Detroit, Michigan

Abstract

The phenoxypropionic acid derivative 2-{4-[(7-chloro-2-quinoxalinyl)oxy]phenoxy}propionic acid (XK469) and an analogue termed 2-{4-[(7-bromo-2-quinalinyl)oxy]phenoxy}-propionic acid (SH80) can eradicate malignant cell types resistant to many common antitumor agents. Colony formation assays indicated that a 24 h exposure of L1210 cells to XK469 or SH80 inhibited clonogenic growth with CI_{90} values of 10 and 13 μmol/L, respectively. This effect was associated with G_2-M arrest and the absence of any detectable markers of apoptosis (i.e., plasma membrane blebbing, procaspase 3 activation, loss of mitochondrial membrane potential, and formation of condensed chromatin). Drug-treated cells increased in size and eventually exhibited the characteristics of autophagy (i.e., appearance of autophagosomes and conversion of microtubule-associated protein light chain 3-I to 3-II). The absence of apoptosis was not related to an inhibition of the apoptotic program. Cultures treated with XK469 or SH80 readily underwent apoptosis upon exposure to the Bcl-2/Bcl-x_L antagonist ethyl 2-amino-6-bromo-4-(1-cyano-2-ethoxy-2-oxoethyl)-4H-chromene-3-carboxylate. Continued incubation of drug-treated cells led to a reciprocal loss of large autophagic cells and the appearance of smaller cells that could not be stained with Höechst dye HO33342, had a chaotic morphology, were trypan blue–permeable, and lacked mitochondrial membrane potential. L1210 cells cotreated with the phosphatidylinositol-3-kinase inhibitor wortmannin, or having reduced Atg7 protein content, underwent G_2-M arrest, but not autophagy, following XK469 treatment. Hence, the therapeutic actions of XK469/SH80 with L1210 cultures reflect both the initiation of a cell cycle arrest as well as the initiation of autophagy. [Mol Cancer Ther 2007;6(1):370–9]

Introduction

2-{4-[(7-Chloro-2-quinoxalinyl)oxy]phenoxy}propionic acid (XK469) is a member of the quinoxaline family of antitumor agents and is an analogue of the herbicide ethyl 2-{4-[(6-chloro-2-quinoxalinyl)oxy]phenoxy}propionate (XK472; also termed Assure; refs 1, 2). A synthetic program has developed additional active drug analogues including an agent designated 2-{4-[(7-bromo-2-quinalinyl)oxy]phenoxy}-propionic acid (SH80; refs. 3, 4). This class of drugs is of potential interest because of their efficacy towards a broad range of human tumor types, including those that express the multidrug resistance phenotype (1–4).

XK469 exhibits several useful therapeutic properties. As a single agent, it has been reported to be cytostatic toward the human U-937, HCT-116, and H460 cell lines via the induction of G_2-M arrest (5–8). It is also highly cytotoxic to a variety of cultured or transplanted human tumor cell lines (1–4, 9, 10). As yet, the nature of the cytotoxic response to XK469 has not been completely characterized. A cell death process consistent with apoptosis was observed in both ovarian tumor cells (9) and cells derived from a Waldenstrom's macroglobulinemia (10). Although the L1210 murine leukemia cell line readily undergoes apoptosis when treated with a variety of proapoptotic agents/procedures (11), we have never observed the development of apoptotic features in this cell line following exposure to XK469.[4]

Macroautophagy is a process in which cytosol and whole organelles become encased in vacuoles (i.e., autophagosomes) that subsequently fuse with lysosomes. In this report, we will use the terms ''autophagy'' and ''macroautophagy'' interchangeably. Following fusion, the contents of the autophagosome are digested and recycled (12–14). Although originally characterized as a survival response to nutrient deprivation, it is now recognized that autophagy is often induced in response to a variety of stressors in order to maintain cellular homeostasis (14–18).

Received 9/26/06; revised 10/30/06; accepted 11/21/06.

Grant support: National Cancer Institute grants CA-082341 (J.P. Horwitz and D. Kessel) and CA-23378 (D. Kessel and J. Reiners). Additional support from the Imaging and Cytometry Facility Core supported by NIEHS grant P30 ES06639 and the Jack and Miriam Schenkman Cancer Research Fund (J.P. Horwitz).

The costs of publication of this article were defrayed in part by the payment of page charges. This article must therefore be hereby marked *advertisement* in accordance with 18 U.S.C. Section 1734 solely to indicate this fact.

Requests for reprints: David Kessel, Department of Pharmacology, Wayne State University School of Medicine, Detroit, MI 48201. Phone: 313-577-1766; Fax: 313-577-6739. E-mail: dhkessel@med.wayne.edu

doi:10.1158/1535-7163.MCT-05-0386

[4] D. Kessel and J.J. Reiners, Jr., unpublished data.

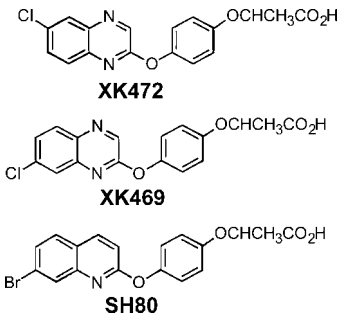

Figure 1. Structures of phenoxypropionic acid derivatives.

The initiation of autophagy can also lead to cell death. Indeed, autophagy mediates regressions of the corpus luteum and Mullerian duct structures, and involution of mammary glands in mammals via selective cell killing (see references within refs. 15, 16). Similarly, the cytotoxicity of some anticancer agents is linked to the induction of autophagy (19–23). Cell death occurring via autophagy has morphologic and biochemical features that distinguish it from both apoptosis and necrosis (reviewed in refs. 15, 16). Furthermore, because autophagy develops in a sequential fashion with multiple levels of regulation, it is currently considered to be a type of programmed cell death (15–18).

In this study, we explored the possibility that XK469 and SH80 kill L1210 cells via the induction of autophagy. As a control, we included analyses of the herbicide XK472 (Assure), a close structural analogue of XK469 (Fig. 1) that lacks antitumor activity (3). We found that L1210 cells treated with cytotoxic concentrations of XK469 or SH80 underwent morphologic and biochemical changes consistent with the induction of autophagy. The herbicide XK472 was inactive in this regard.

Materials and Methods

Cell Lines and Culture Conditions

Murine L1210 cells were maintained in suspension culture using the formulation of Fisher's growth medium. This was obtained by supplementing α-MEM (Life Technologies, Grand Island, NY) with $MgCl_2$ (45 mg/L), methionine (75 mg/L), phenylalanine (30 mg/L), valine (30 mg/L), and folic acid (9 mg/L). Additional components were 10% horse serum, 1 mmol/L glutamine, 1 mmol/L mercaptoethanol, and gentamicin. Cultures were incubated with specified agents for 24 to 240 h at 37°C. Viability was determined by a clonogenic procedure with colonies counted after 7 to 10 days. Cell size was determined with a Coulter particle analyzer communicating with a model 256 Channelyzer.

Chemicals

Stock solutions of XK472, R(+)XK469 and R(+)SH80 were prepared in DMSO at a 10 mmol/L concentration. These were diluted into cell cultures to achieve specified drug concentrations. XK472 was a gift from the DuPont-Merck Pharmaceutical Company (Wilmington, DE). The other agents were synthesized as previously described (3, 4). Höechst dye HO33342 (HO342) and tetramethylrhodamine methyl ester (TMRM) were purchased from Molecular Probes (Carlsbad, CA). The Bcl-2 antagonist ethyl 2-amino-6-bromo-4-(1-cyano-2-ethoxy-2-oxoethyl)-4H-chromene-3-carboxylate (HA14-1) was provided by Ryan Scientific, Inc. (Isle of Palms, SC). Wortmannin was obtained from Sigma Chemical, Co. (St. Louis, MO).

Assay of Caspase 3/7 Activities

Control cells and cells previously treated with XK472, XK469, or SH80 for 24 or 48 h were washed, and then lysed in 200 μL of buffer containing 50 mmol/L of Tris (pH 7.2), 0.03% Nonidet P40, and 1 mmol/L of DTT. The lysate was briefly sonicated and the debris removed by centrifugation at 10,000 × *g* for 1 min. The supernatant fluid (100 μL) was mixed with 40 μmol/L of DEVD-R110, 10 mmol/L of HEPES (pH 7.5), 50 mmol/L of NaCl, and 2.5 mmol/L of DTT in a total volume of 200 μL. The rate of increase in fluorescence emission, resulting from the release of rhodamine-110 from the fluorogenic substrate zDEVD-R110 (24) was measured over 30 min at room temperature, using a fluorescence plate reader. DEVDase activity is reported in terms of nmol product/min/mg protein.

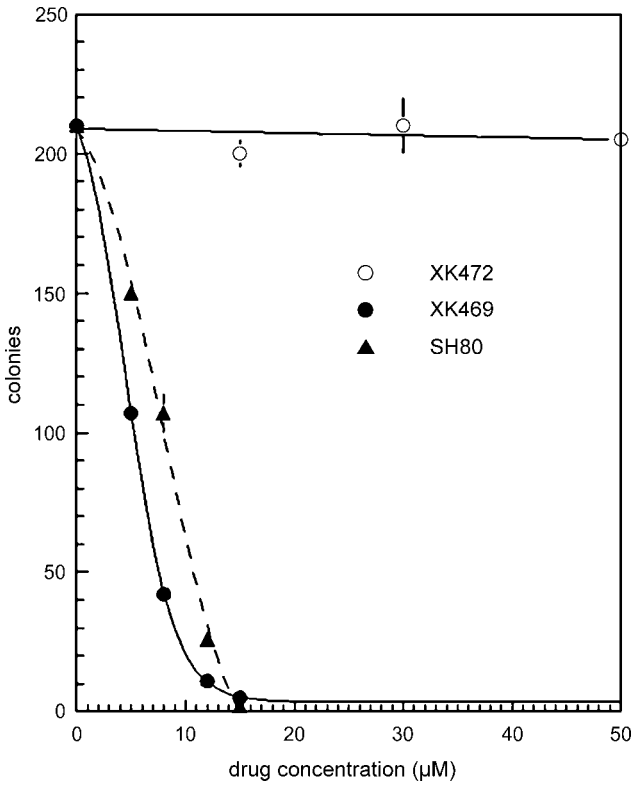

Figure 2. Colony formation following phenoxypropionic acid analogue treatment. Cultures of L1210 cells were treated with varied concentrations of XK472, XK469, and SH80 for 24 h prior to being plated for analyses of colony formation. *Points,* means of three plates; *bars,* SD.

Control determinations were made on extracts of untreated cells. Each assay was done with triplicate samples. The Bio-Rad assay (Hercules, CA), using bovine serum albumin as a standard, was used to estimate protein concentrations.

The Bcl-2/Bcl-x_L antagonist HA14-1 (25) was used to test the ability of drug-treated cells to undergo apoptosis. For this purpose, cells were first incubated with a CI_{90} level of XK469 or SH80 for 24 h, and then exposed to 40 μmol/L of HA14-1 for 1 h at 37°C prior to harvesting for analyses of DEVDase. A comparison was made using cultures that had been treated for 1 h with only HA14-1.

Flow Cytometry

L1210 cells were harvested and processed for fluorescence-activated cell sorting analysis of DNA content as described previously (26). DNA analyses were made with a BD Biosciences FACScalibur instrument (San Jose, CA). Percentages of cells in G_0-G_1, S, and G_2-M stages of the cell cycle were determined with a DNA histogram-fitting program (MODFIT; Verity Software, Topsham, ME). A minimum of 2×10^4 events/sample were collected for subsequent analyses.

Western Blot Analysis

After the specified treatments, cells were lysed in SDS-PAGE buffer and lysate was heated to 100°C for 5 min and then used for Western blot analysis. Similar amounts of protein (usually 40 μg) were analyzed in each lane. Electrophoresis was carried out on 4% to 20% acrylamide gels and the proteins were transferred to polyvinylidene fluoride membranes. After washing and blocking, the membranes were incubated overnight at 4°C with a rabbit polyclonal caspase 3 antibody (BD PharMingen, San Diego, CA), a rabbit polyclonal antibody raised to microtubule-associated protein light chain 3 (LC3; kindly provided by Dr. Masahiro Shibata, Department of Cell Biology and Neuroscience, Osaka University Graduate School of Medicine, Japan), or a rabbit polyclonal antibody made to a peptide mapping to the COOH terminus of human Atg7 (Prosci, Inc., Poway, CA), or a goat polyclonal antibody raised against a peptide mapping to the COOH terminus of human actin (Santa Cruz Biotechnology, Inc., Santa Cruz, CA). After washing, the membranes were incubated for 1 h with alkaline phosphatase–coupled, species appropriate secondary antibody at room temperature. Immunofluorescence signals were detected with Vistra ECF Western blot reagent (Amersham Biosciences, Corp., Piscataway, NJ) using the Storm imaging system (Molecular Dynamics, Sunnyvale CA).

Atg7 Gene – Silencing Methodology

A retroviral vector that encoded a short hairpin RNA construct directed against murine Atg7 was obtained from Open Biosystems (Huntsville, AL). A scrambled nonsilencing short hairpin RNA pSM2 vector was also obtained from Open Biosystems. The latter short hairpin RNA sequence is expressed under the control of the U6 promoter and contains no homology to known mammalian genes. L1210 cells were transfected using LipofectAMINE (Invitrogen, Carlsbad, CA), and stables were selected on the basis of their resistance to puromycin. Cultures were periodically monitored by Western blotting to ensure continued silencing of Atg7.

Microscopy

Phase contrast and fluorescence images were acquired using a Nikon Eclipse E600 microscope and a CCD camera (Photometrics, Tucson, AZ). Images were processed using MetaMorph software (Universal Imaging, Downington, PA). In all studies, a cooled microscopy stage operating at

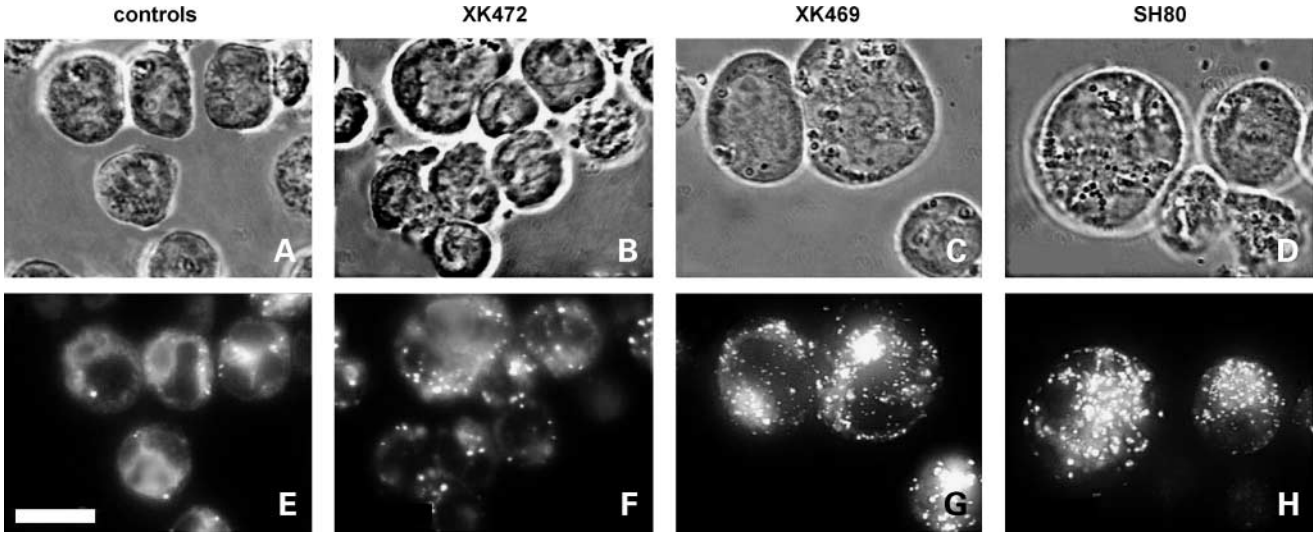

Figure 3. XK469 and SH80 stimulation of vacuolization and formation of monodansylcadaverine-labeled vesicles. L1210 cells were treated with nothing, 50 μmol/L of XK472, or a CI_{90} concentration of XK469 or SH80 for 24 h prior to being viewed by phase contrast microscopy (*top row*) or stained with monodansylcadaverine and imaged by fluorescence microscopy (*bottom row*). **A** and **E**, controls; **B** and **F**, XK472; **C** and **G**, XK469; **D** and **H**, SH80. *Bar*, 10 μm.

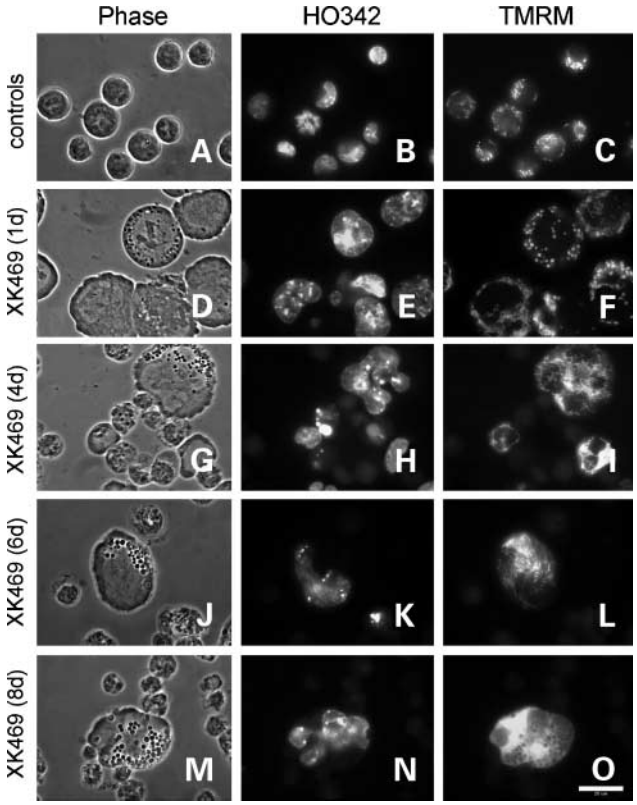

Figure 4. Kinetic analyses of effects of XK469 on morphology, chromatin condensation, and mitochondrial membrane potential. L1210 cultures were treated with nothing or a CI_{90} concentration of XK469 for 1, 4, 6, or 8 d prior to being viewed by phase contrast microscopy (*left*), stained with HO342 (*center*), or TMRM (*right*) and imaged by fluorescence microscopy. **A** to **C**, controls; **D** to **F**, XK469 (1 d); **G** to **I**, XK469 (4 d); **J** to **L**, XK469 (6 d); **M** to **O**, XK469 (8 d). *Bar*, 20 μm.

15°C was employed to prevent metabolic changes during observation. Some fluorescence images were collected using a Z-drive and AutoQuant deconvolution software in order to obtain maximal pixel representation. A Uniblitz shutter controlled the exposure of cells to the excitation source. This was configured to open and close with the camera shutter to minimize photobleaching. Phase contrast images were acquired from single planes with no image deconvolution.

To assess changes in morphology after XK469 or SH80 treatment, cells were incubated with an LD_{90} level of either drug for specified times. Samples of these cultures were examined at daily intervals. Fluorescent probes used were HO342 (3 μmol/L, 5 min incubation at 37°C) for examination of nuclear morphology, TMRM to assess the mitochondrial membrane potential (1 μmol/L, 10 min exposure), and monodansylcadaverine for imaging of lysosomes and autophagic vacuoles (25 μmol/L, 30 min treatment). HO342 and TMRM have been used as probes for apoptotic phenomena in previous studies (11). Monodansylcadaverine is a marker for lysosomal activity and fused autolysosomes (15, 27, 28). After labeling, cells were washed once with 0.9% NaCl and examined by fluorescence microscopy. Excitation wavelengths were 360 to 380 nm (HO342, monodansylcadaverine) and 510 to 560 nm (TMRM). Interference filters were used to isolate the emission fluorescence of HO342 (400–450 nm), monodansylcadaverine (520–560 nm), and TMRM (550–650 nm). Because of the absence of spectral overlap, it was feasible to visualize HO342 and TMRM fluorescence in the same field.

For electron microscopy, L1210 cells were fixed with glutaraldehyde and osmium tetroxide, treated with uranyl acetate + lead citrate for enhanced protein and lipid staining, and then dehydrated in ethanol. The cell pellets were embedded in epon resin and cut with an ultramicrotome to a 70 nm thickness before viewing.

Results

Phenoxypropionic Acid Effects on Cell Viability, Size, and Morphology

Concentrations of XK472 ≤ 50 μmol/L affected neither L1210 viability (Fig. 2) nor cell morphology (data not presented). In contrast, clonogenic assays suggested that similar concentrations of XK469 and SH80 were highly cytostatic/cytotoxic (Fig. 2). CI_{90} concentrations for XK469 and SH80 were found to be 10 and 13 μmol/L, respectively (Fig. 2). Mean cell size increased substantially after exposure of cells to a LD_{90} concentration of these agents for 24 h. Analyses with a Coulter Channelyzer indicated that with XK469, the mean diameter increased from 12.1 ± 1.2 to 14.6 ± 1.6 μm in 24 h, indicating a 1.76-fold volume increase. After exposure to SH80, the average diameter increased to 15.2 ± 1.4 μm for a 2-fold increase in volume.

Phase contrast microscopy confirmed the enlargement of L1210 cells following 24 h of exposure to LD_{90} concentrations of either XK469 or SH80 (compare Fig. 3A with C and D). In contrast, cell size was not affected by exposure to 50 μmol/L of XK472 (compare Fig. 3A and B). Figure 4 depicts the effects of XK469 exposure on L1210 size over 8 days. A majority of the cells were significantly enlarged within 24 h of XK469 exposure (compare Fig. 4A and D). A portion of this population remained enlarged following 7 additional days of culture (Fig. 4G, J, and M). Vacuoles became apparent in some enlarged cells within 24 h of treatment, and every enlarged cell was vacuolated within 96 h of treatment. The enlarged cells maintained their mitochondrial membrane potential ($\Delta\Psi_m$), as indicated by TMRM staining throughout the 8-day period (Fig. 4F, I, L, and O). Interestingly, in some 24-h XK469–treated cells, TMRM staining colocalized with vacuoles (compare Fig. 4D and F). However, by 96 h of treatment, this colocalization was lost. After the initial 24 h treatment period, there occurred a progressive loss of enlarged cells, and the reciprocal appearance of a cell population that was smaller, had a chaotic morphology, lacked $\Delta\Psi_m$, and was not stainable with HO342 (Fig. 4). Analyses of several fields of cells (≥100 cells total) revealed that ~65% of the cell population was enlarged and vacuolated, with the remainder shrunken and chaotic after 48 h of XK469 treatment. After 72 h, these numbers were reversed, with 35% enlarged and vacuolated, and 65%

Table 1. Effects of XK469 analogues, wortmannin, and Atg7 deficiency on cell cycle progression

Treatment	Elapsed time (h)	Cells in designated phase (%)		
		G_0-G_1	S	G_2-M
Experiment 1				
Solvent	24	47	40	13
	48	49	35	16
XK472	24	54	31	14
	48	53	32	15
XK469	24	10	31	59
	48	11	23	66
SH80	24	14	27	59
	48	16	24	60
Experiment 2				
Solvent	24	35	55	10
	48	38	51	11
	72	43	47	10
Wortmannin	24	36	53	11
	48	37	51	12
	72	47	42	10
XK469	24	10	40	50
	48	1	27	72
	72	5	23	72
XK469 + wortmannin	24	8	50	42
	48	3	37	60
	72	4	24	72
Experiment 3				
WT-L1210	48	40	50	10
WT-L1210 + XK469	24	3	40	57
	48	2	18	80
	72	3	24	73
Atg7-L1210 + XK469	24	6	29	65
	48	3	18	79
	72	6	21	73

NOTE: In experiment no. 1, L1210 cultures were treated with solvent, 50 μmol/L of XK472 or CI_{90} concentrations of XK469 or SH80 for the indicated amounts of time prior to being harvested for analysis of DNA contents by flow cytometry. In experiment no. 2, L1210 cultures were treated with solvent, 100 nmol/L of wortmannin, a CI_{90} concentration of XK469 or XK469 + wortmannin for the indicated lengths of time before harvesting. In experiment no. 3, wild-type or Atg7-deficient L1210 cultures were treated with a CI_{90} concentration of XK469 for the indicated lengths of time before harvesting.

shrunken and chaotic. After 8 days, >95% of the cells were shrunken and chaotic. The shrunken cells were permeable to trypan blue, whereas even after 8 days, the enlarged cells were trypan blue–impermeable.

Cell Cycle Analysis

Exposure of L1210 cultures to 50 μmol/L of XK472 for 24 to 48 h had no effects on cell cycle progression (Table 1, experiment 1). In contrast, exposure of cultures to a CI_{90} concentration of either XK469 or SH80 resulted in dramatic losses of G_1 phase cells and reciprocal accumulations of G_2-M phase cells. Cell counting analyses indicated that L1210 cultures treated with a CI_{90} concentration of either XK469 or SH80 were effectively arrested (at most, one doubling within 96 h).

Procaspase 3 Activation

The morphologic characteristics of XK469- or SH80-treated cultures were not consistent with cells undergoing apoptosis. DEVD-R110 is a substrate for caspases-3 and -7. Caspase-dependent DEVDase activities (defined as being inhibited by zDEVD-fmk) were comparable in control cultures, cultures treated with 50 μmol/L XK472, or with CI_{90} concentrations of either XK469 or SH80 (Table 2). Western blot analyses of procaspase processing also indicated that these agents did not stimulate procaspase 3 activation (Fig. 5A). In contrast, procaspase 3 was rapidly activated in L1210 cells treated with the proapoptotic Bcl-2 small molecule antagonist HA14-1 (Table 2; Fig. 5A, *lane HA*). Furthermore, DEVDase activities could be induced in cultures pretreated for 24 or 48 h with XK469 or SH80 if the cultures were cotreated with HA14-1 for 1 h prior to harvest (Table 2).

An additional study was done to show HA14-1 induction of an apoptotic response in cultures previously exposed to XK469. No apoptotic nuclei (as monitored by HO342 staining) were detected in L1210 cultures following a 24 h exposure to a CI_{90} concentration of XK469 (Fig. 5B). However, nuclei with condensed chromatin appeared within 1 h of the addition of 40 μmol/L of HA14-1 (Fig. 5C). Hence, the absence of an apoptotic response in XK469- or SH80-treated cultures was not due to an inhibition of the apoptotic program by either drug.

Characterization of Autophagy

The morphologic changes occurring in L1210 cells following XK469 or SH80 treatment (i.e., cell enlargement and development of vacuoles) were consistent with the development of an autophagic response. The fluorescent compound monodansylcadaverine is commonly used to stain autophagic vesicles (15, 27, 28). Control and XK472 cells exhibit diffuse monodansylcadaverine staining throughout the cytoplasm, and a few, strongly stained punctate areas (Fig. 3E and F). A 24-h treatment with a CI_{90}

Table 2. Effects of XK469 and SH80 on DEVDase activation

Conditions	DEVDase (nmol/min/mg protein)		
	60 min	24 h	48 h
Control	0.08 ± 0.03	0.12 ± 0.06	0.15 ± 0.04
HA14-1	4.42 ± 0.48	—	—
XK472	—	0.12 ± 0.05	0.15 ± 0.07
XK469	—	0.18 ± 0.07	0.17 ± 0.05
SH80	—	0.20 ± 0.05	0.22 ± 0.07
XK472/HA14-1	—	4.13 ± 0.40	3.28 ± 0.47
XK469/HA14-1	—	3.98 ± 0.52	1.38 ± 0.37
SH80/HA14-1	—	4.10 ± 0.47	2.90 ± 0.30

NOTE: In the first five treatment rows, cultures were treated with nothing, 40 μmol/L of HA14-1, or 50 μmol/L of XK472, or CI_{90} concentrations of XK469 or SH80 for the indicated times prior to being harvested. In the bottom three rows, cultures were exposed to 50 μmol/L of XK472 or CI_{90} concentrations of XK469 or SH80 for the indicated times plus HA14-1 during the last hour of incubation. Data represents the results of three experiments (mean ± SD).

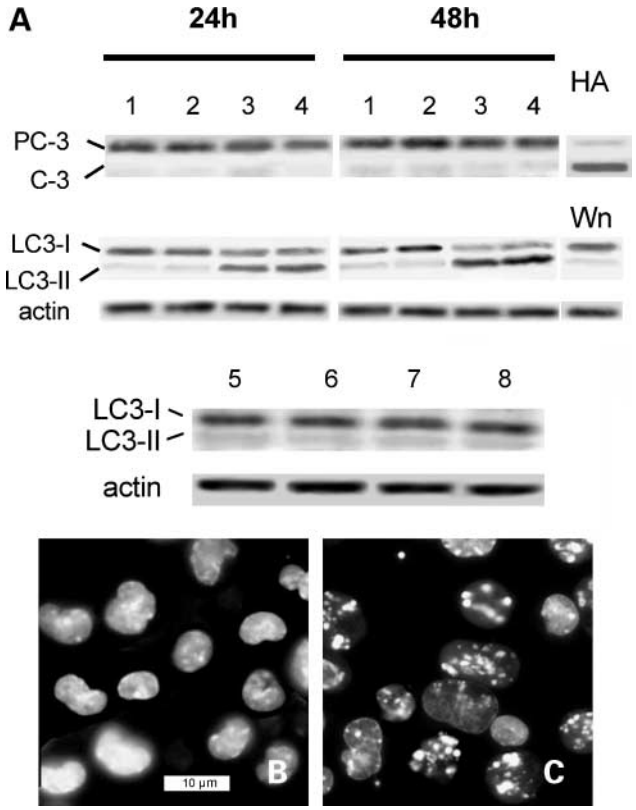

Figure 5. Induction of apoptosis and LC3 processing by phenoxypropionic acid analogues. **A,** Western blot analyses of procaspase 3 activation (*top*) and LC3-I processing (*bottom*). L1210 cultures were treated with nothing (*1*), 50 μmol/L of XK472 (*2*), CI_{90} concentrations of XK469 (*3*) or SH80 (*4*) for 24 or 48 h prior to being harvested for Western blot analyses of procaspase 3 (*PC-3*) conversion to caspase 3 (*C-3*), or LC3-I conversion to LC3-II. *HA,* cultures treated with 40 μmol/L of HA14-1 for 1 h prior to harvest. *Wm,* cultures that were coincubated for 24 h with a CI_{90} concentration of XK469 and 100 nmol/L of wortmannin. *Lanes 5* to *8,* a similar study involving 24-h exposure of Atg7-deficient cells: (*5*) control, (*6*) 50 μmol/L of XK472, (*7*) CI_{90} of XK469, and (*8*) CI_{90} of SH80. Analyses are of 40 μg of cell lysate. *Bottom,* L1210 cultures were treated with a CI_{90} concentration of XK469 for 24 h either in the absence (**B**) or presence (**C**) of 40 μmol/L of HA14-1 (present during the final 60 min) prior to staining with HO342.

concentration of either XK469 (Fig. 3G) or SH80 (Fig. 3H) dramatically increased the number of strongly stained punctate areas.

Microtubule-associated protein LC3 is a structural and functional human homologue of the yeast gene *Atg8*, the protein product of which is required for autophagy (29, 30). Shortly after translation, microtubule-associated protein LC3 is cleaved to yield a protein termed LC3-I (30–32). Upon the induction of autophagy, LC3-I is covalently linked to phosphatidylethanolamine to yield phosphatidylethanolamine-modified LC3-II, which associates with the autophagosome (30–32). The presence of phosphatidylethanolamine on LC3-II makes it migrate more rapidly than LC3-I on SDS denaturing gels (29, 32). Although both LC3-I and LC3-II were detectable in nontreated and XK472-treated cultures (Fig. 5A), the LC3-I form was the predominant species. This changed after treatment with either XK469 or SH80. The LC3-II form became the predominant species within 48 h of treatment, and its appearance was paralleled by the loss of the LC3-I form (Fig. 5A).

A defining feature of the autophagosome is a double-walled membrane (32). Figure 6 depicts an electron micrograph of a typical L1210 cell following 24 h of exposure to an LD_{90} concentration of XK469. Multiple vacuoles can be seen within a cell. An enlargement of one of the vacuoles clearly shows that it is encased within a double membrane, and that it contains a smaller autophagosome.

Pharmacologic Suppression of Autophagy

The development of autophagy is dependent on class III phosphatidylinositol-3-kinase activity (28, 33). This activity can be pharmacologically inhibited by wortmannin (34). Coincubation of L1210 cultures with 100 nmol/L of wortmannin modestly inhibited XK469-induced cell

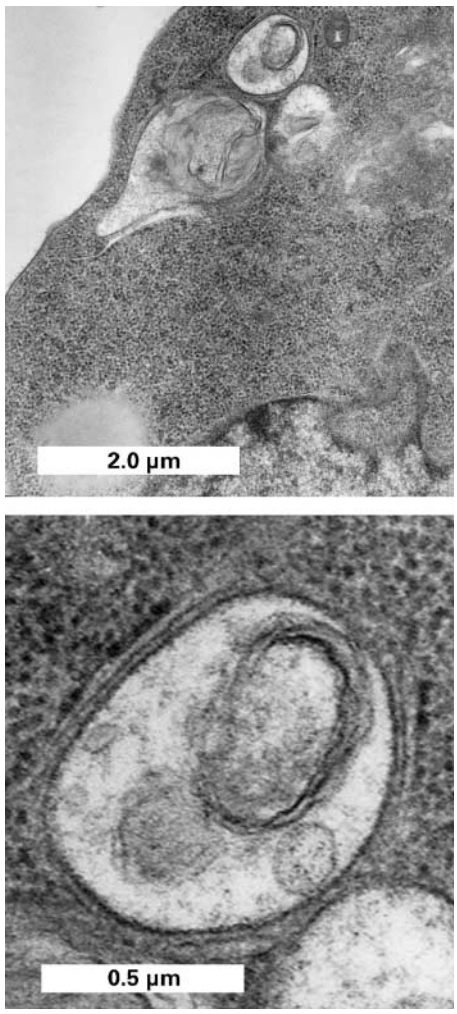

Figure 6. Electron micrographs of an L1210 cell after a 24 h exposure to a CI_{90} concentration of XK469. *Bottom,* a typical vacuole. Original magnifications, ×5,000 (*top*); ×30,000 (*bottom*).

enlargement (compare Fig. 7A with C and E), but had no effect on the induction of a G_2-M phase arrest (Table 1, experiment 2). However, wortmannin cotreatment suppressed XK469 vacuolization (compare Fig. 7B with C and Fig. 7D with E), and delayed the appearance of shrunken cells that failed to stain with HO342 (compare top with bottom rows in Fig. 7). Cotreatment with wortmannin also suppressed XK469-mediated conversion of LC3-I to LC3-II (Fig. 5A, *lane Wn*).

Effects of Atg7 Silencing

The product of the *Atg7* gene is required for autophagosome generation (35, 36). Transfection and selection of cells that expressed short hairpin RNA directed against Atg7 mRNA resulted in a significant knockdown of endogenous Atg7 protein levels (compare Fig. 8A and B).

Untreated L1210 cells with reduced Atg7 levels were morphologically similar, and comparable in size to the parental line (Fig. 8C and F). Similar to wild-type L1210 cultures, Atg7-deficient cells arrested in G_2-M following 24 to 72 h of exposure to XK469 (Table 1, experiment 3). Atg7-deficient cells became enlarged following exposure to XK469 or SH80 (compare Fig. 8C, F, I, and L). However, unlike XK469- or SH80-treated wild-type L1210 cells, similarly treated Atg7-deficient cells were neither vacuolated nor gave rise to the smaller, trypan blue–permeable, $\Delta\Psi_m$-deficient, non–HO342-stainable cell population (compare Fig. 8I–N with Fig. 4D–F and G–I). Moreover, LC3 processing was not observed after treatment of Atg7-deficient cells with XK469 or SH80 (Fig. 5A, *lanes 5–8*). L1210 cells stably transfected with a scrambled short hairpin RNA vector, like the parental cell line, developed autophagic characteristics following treatment with XK469 (compare Fig. 8O–Q with Fig. 7D and I).

Discussion

Autophagy is a process whereby double membrane vacuoles termed autophagosomes form around, and engulf, cytosol and organelles (12, 13). Subsequent fusion with lysosomes enables degradation of autophagosome contents. Autophagy is the mechanism whereby cells degrade/recycle damaged/aged organelles, and constitutes a normal physiologic response to nutrient deprivation, and some forms of stress (13–15). As such, autophagy functions as a prosurvival response. However, it is also clear that the cytotoxicity of some stressors is mediated via their induction of autophagy. For example, the cytotoxicity of tamoxifen (23), arsenic trioxide (21), endostatin (22), and ionizing radiation (20) to some cell types is mediated by the induction of autophagy, not apoptosis. In such situations, autophagy constitutes a nonapoptotic pathway for programmed cell death.

The traits of cells undergoing apoptosis or autophagy are markedly different, and have been recently reviewed (15, 16). During apoptosis, a variety of procaspases are activated, cells shrink, and exhibit both condensed nuclear chromatin and sub-G_1/G_0 DNA contents. These traits are

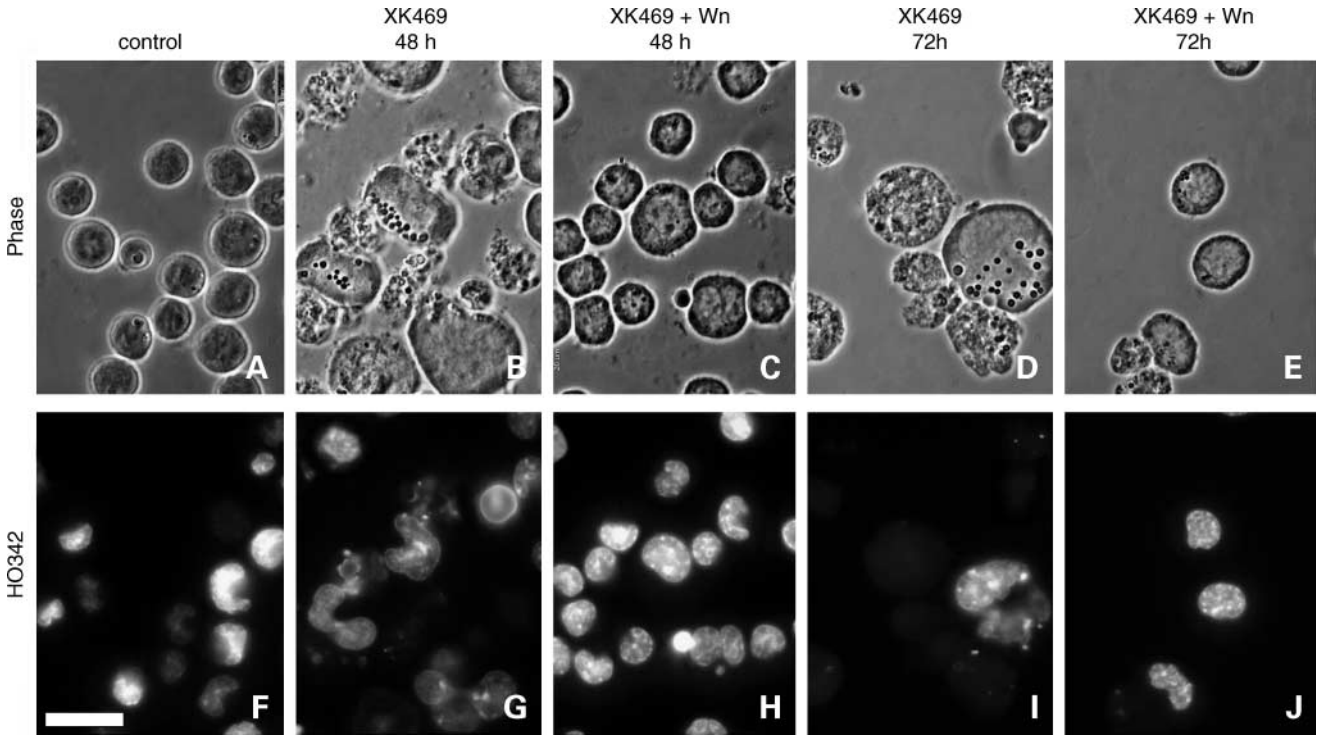

Figure 7. Suppression of XK469-induced autophagy by wortmannin. L1210 cultures were treated with nothing (**A** and **F**), or with a CI_{90} concentration of XK469 for 48 h in the absence (**B** and **G**) or presence of 100 nmol/L of wortmannin (**C** and **H**), or for 72 h in the absence (**D** and **I**) or presence of wortmannin (**E** and **J**). Cultures were analyzed by phase contrast microscopy (*top row*) or stained with HO342 and viewed by fluorescence microscopy (*bottom row*). *Bar,* 20 μm.

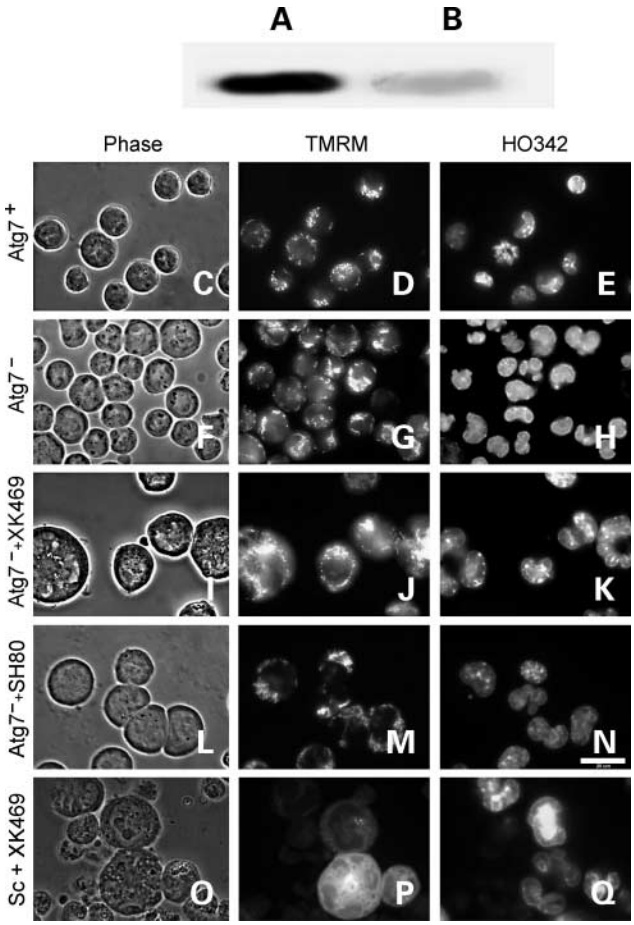

Figure 8. Suppression of XK469- and SH80-induced autophagy by Atg7 deficiency. *Top,* Western blot analyses of Atg7 in wild-type (**A**) and Atg7-deficient (**B**) L1210 cultures. Analyses are of 40 μg of cell lysate. *Bottom,* wild-type (**C – E**), Atg7-deficient (**F – N**), or scramble sense transfected (**O – Q**) L1210 cells were either left untreated (**C – H**), or treated with a CI_{90} concentration of XK469 (**I – K** and **O – Q**), or SH80 (**L – N**) for 72 h prior to being viewed by phase contrast microscopy (*left*), stained with TMRM (*middle*), or HO342 (*right*), and imaged by fluorescence microscopy. *Bar,* 20 μm.

not seen in cells undergoing autophagy. Conversely, cells undergoing autophagy generally enlarge without permeabilization of the plasma membrane, convert LC3-I to LC3-II, exhibit enhanced monodansylcadaverine labeling, and develop unique vacuoles (i.e., autophagosomes) that have a double-walled membrane. In the current study, L1210 cultures treated with CI_{90} concentrations of XK469 or SH80 exhibited morphologic and biochemical features that are characteristic of cells undergoing autophagy, not apoptosis. The observations that Atg7 and class III phosphatidylinositol-3-kinase deficiency (as a consequence of wortmannin treatment) suppressed the development of autophagic traits also support our conclusion that XK469/SH80 induces autophagy in L1210 cultures.

Although the role of autophagy as a death mode has been argued (37, 38), the results described here are consistent with the proposal that XK469 and SH80 kill L1210 cells via an autophagic pathway. Although autophagy developed quickly following XK469/SH80 treatment, the subsequent death of exposed cells was not rapid. Within 24 h of XK469 exposure, most cells had enlarged and developed autophagosomes. Over the next 7 days, there appeared a second population of cells that were shrunken, had a chaotic morphology, exhibited minimal HO342 labeling, lacked $\Delta\Psi_m$, and were trypan blue–permeable. We conclude that this population was derived from the larger autophagic population because (*a*) cell numbers did not increase following XK469/SH80 treatment, (*b*) the appearance of the smaller cells correlated with a reciprocal loss of the larger cell population, and (*c*) cells with the characteristics of the smaller cell population did not appear in cultures in which the formation of the initial large, autophagic population was blocked due to either Atg7 deficiency or wortmannin treatment. We propose that this population of smaller, dye-permeable cells died via an autophagic process. Although Atg7-deficient cells did not exhibit autophagic properties following 72 h of XK469 treatment, they were arrested in G_2-M. Clonogenic assays indicated that these cells did not recover from the cytostatic effects of drug treatment.

A limited number of studies have reported that XK469 can induce apoptosis in some cell lines (9, 10). Although L1210 cells readily undergo apoptosis following exposure to a variety of stressors (11), we observed no indications of apoptosis following XK469/SH80 treatment. The mechanism whereby XK469 and SH80 evoke autophagy, but not apoptosis, in L1210 cells is unknown. However, the ability of HA14-1 to induce apoptosis in XK469/SH80-treated L1210 cultures eliminates the possibility that the latter agents suppress the apoptotic program in this cell line. In a recent study of six leukemia cell lines, XK469 provoked dramatic losses of the phosphorylated form of S6 ribosomal protein in those lines most sensitive to the drug (39). It was noted that the sensitive cell lines did not die by an apoptotic mechanism. Although the authors made no mention of the involvement of autophagy, conditions leading to ribosomal protein S6 phosphorylation generally suppress autophagy; whereas conditions that suppress S6 phosphorylation generally favor autophagy (13, 15, 40–42). It is also conceivable that the observed autophagy in the current studies reflects a response to XK469-induced organelle damage. In the study depicted in Fig. 4, TMRM staining colocalized to XK469-induced vacuoles at the 24-h treatment point. Presumably, this reflects mitochondria that have been engulfed in autophagosomes. Although speculative, it is conceivable that XK469 may affect mitochondrial function. Lemasters has shown that damaged mitochondria are often earmarked for removal by autophagy (43, 44).

XK469 and SH80 induced a protracted G_2-M arrest in L1210 cultures. This effect was independent of XK469/SH80-induced autophagy because it also occurred in cultures in which the development of autophagy was blocked due to either Atg7 deficiency or cotreatment with wortmannin. Indeed, the ability of XK469 to induce G_2-M arrest may be a general property of the agent, as it also

occurred in XK469-treated U-937, HCT-116, and H460 cultures (5, 6, 9, 10). Analyses of HCT-116 cultures indicated that XK469 suppressed the ubiquitination of cyclin B, a process necessary for proteasome-mediated degradation and progression through metaphase (5).

In summary, the current studies show that XK469, and its analogue, SH80, seem to eradicate L1210 murine leukemia cells via the induction of autophagy. To the best of our knowledge, this is the first report to define such an activity for these compounds. It should be noted that this activity of XK469 is not unique to L1210 cells. We have also observed similar effects in a murine hepatoma cell line.[5] Because the death programs associated with apoptosis and autophagy differ, agents capable of inducing cytotoxicity via the autophagic pathway might be useful in the treatment of tumors that are refractory to inducers of apoptosis. There may also be an additional therapeutic benefit associated with the induction of autophagy. Specifically, autophagic cells exhibit an enhanced presentation of MHC class II antigens derived from cytosolic proteins (45). Autophagy could thereby promote immunologic recognition and elimination of tumor cells.

[5] J.J. Reiners, Jr., unpublished data.

References

1. Corbett TH, LoRusso PM, Demchik L, et al. Preclinical antitumor efficacy of analogues of XK469: sodium 2-{4-[(7-chloro-2-quinoxalinyl)oxy]phenoxy}proprionate. Invest New Drugs 1998;16:129 – 39.
2. LoRusso PM, Parchment R, Demchik L, et al. Preclinical antitumor activity of XK469 (NSC656889). Invest New Drugs 1999;16:287 – 96.
3. Hazeldine ST, Polin L, Kushner J, et al. Design, synthesis and biological evaluation of analogues of the antitumor agent, 2-{4-[(7-chloro-2-quinoxalinyl)oxy]phenoxy}propionic acid (XK469). J Med Chem 2001; 44:1758 – 76.
4. Hazeldine ST, Polin L, Kushner J, et al. Synthesis and biological evaluation of some bioisosteres and congeners of the antitumor agent, 2-{4-[(7-chloro-2-quinoxalinyl)oxy]phenoxy}propionic acid (XK469). J Med Chem 2002;45:3130 – 7.
5. Lin H, Subramanian B, Nakeff A, Chen BD. XK469, a novel antitumor agent, inhibits signaling by the MEK/MAPK signaling pathway. Cancer Chemother Pharmacol 2002;49:281 – 6.
6. Ding Z, Parchment RE, LoRusso PM, et al. The investigational new drug XK469 induces G_2/M cell cycle arrest by p53-dependent and -independent pathways. Clin Cancer Res 2001;7:3336 – 42.
7. Lin H, Liu XY, Subramanian B, Nadeff A, Valeriote F, Chen BD. Mitotic arrest induced by XK469, a novel antitumor agent, is correlated with the inhibition of cyclin B1 ubiquitination. Int J Cancer 2002;97:121 – 8.
8. Ling ZH, Du H, Yuan CQ, Ma SD, Zheng L, Ding ZH. Effect of XK469 and adriamycin on the growth of H460 cells *in vitro* and its mechanism. Di Yi Jun Yi Da Xue Xue Bao 2004;24:775 – 8.
9. Ding Z, Zhou JY, Wei WZ, Baker VV, Wu GS. Induction of apoptosis by the new anticancer drug XK469 in human ovarian cancer cell lines. Oncogene 2002;21:4530 – 8.
10. Mensah-Osman E, Al-Katib A, Dandashi M, Mohammad R. XK469, a topo IIβ inhibitor, induces apoptosis in Waldenstrom's macroglobulinemia through multiple pathways. Int J Oncol 2003;23:1637 – 44.
11. Kessel D, Reiners JJ, Jr. Apoptotic response to photodynamic therapy versus the Bcl-2 antagonist HA14-1. Photochem Photobiol 2002;76:314 – 9.
12. Klionsky DJ. The molecular machinery of autophagy: unanswered questions. J Cell Sci 2005;118:7 – 18.
13. Klionsky DJ, Emr SD. Autophagy as a regulated pathway of cellular degradation. Science 2000;290:1717 – 21.
14. Shintani T, Klionsky DJ. Autophagy in health and disease: a double-edged sword. Science 2004;306:990 – 5.
15. Gozuacik D, Kimchi A. Autophagy as a cell death and tumor suppressor mechanism. Oncogene 2004;23:2891 – 906.
16. Debnath J, Baehrecke EH, Kroemer G. Does autophagy contribute to cell death? Autophagy 2005;1:66 – 74.
17. Nelson DA, White E. Exploiting different ways to die. Genes Dev 2004;18:1223 – 5.
18. Edinger AL, Thompson CB. Death by design: apoptosis, necrosis and autophagy. Curr Opin Cell Biol 2004;16:663 – 9.
19. Ito H, Daido S, Kanzawa T, Kondo S, Kondo Y. Radiation-induced autophagy is associated with LC3 and its inhibition sensitizes malignant glioma cells. Int J Oncol 2005;26:1401 – 10.
20. Paglin S, Hollister T, Delohery T, et al. A novel response of cancer cells to radiation involves autophagy and formation of acidic vesicles. Cancer Res 2001;61:439 – 44.
21. Kanzawa T, Kondo Y, Ito H, Kondo S, Germano I. Induction of autophagic cell death in malignant glioma cells by arsenic trioxide. Cancer Res 2003;63:2103 – 8.
22. Chau YP, Lin SY, Chen JH, Tai MH. Endostatin induces autophagic cell death in EAhy926 human endothelial cells. Histol Histopathol 2003; 18:715 – 26.
23. Bursch W, Ellinger A, Kienzl H, et al. Active cell death induced by the anti-estrogens tamoxifen and ICI 164 384 in human mammary carcinoma cells (MCF-7) in culture: the role of autophagy. Carcinogenesis 1996;17: 1595 – 607.
24. Cai SX, Zhang HZ, Guastella J, Drewe J, Yang W, Weber E. Design and synthesis of rhodamine 110 derivative and caspase-3 substrate for enzyme and cell-based fluorescent assay. Bioorg Med Chem Lett 2001;11: 39 – 42.
25. Wang JL, Liu D, Zhang ZJ, et al. Structure-based discovery of an organic compound that binds Bcl-2 protein and induces apoptosis of tumor cells. Proc Natl Acad Sci U S A 2000;97:7124 – 9.
26. Reiners JJ, Jr., Clift R, Mathieu P. Suppression of cell cycle progression by flavonoids: dependence on the aryl hydrocarbon receptor. Carcinogenesis 1999;20:1561 – 6.
27. Biederbick A, Kern HF, Elsasser HP. Monodansylcadaverine (MDC) is a specific *in vivo* marker for autophagic vacuoles. Eur J Cell Biol 1995;66: 3 – 14.
28. Munafo DB, Colombo MI. A novel assay to study autophagy: regulation of autophagosome vacuole size by amino acid deprivation. J Cell Sci 2001;114:3619 – 29.
29. Kirisako T, Baba M, Ishihara N, et al. Formation process of autophagosome is traced with Apg8/Aut7p in yeast. J Cell Biol 1999; 147:435 – 46.
30. Kabeya Y, Mizushima N, Ueno T, et al. LC3, a mammalian homologue of yeast Apg8p, is localized in autophagosome membranes after processing. EMBO J 2000;19:5720 – 8.
31. Kabeya Y, Mizushima N, Yamamoto A, Oshitani-Okamoto S, Ohsumi Y, Yoshimori T. LC3, GABARAP and Gate16 localize to autophagosomal membrane depending on form-II formation. J Cell Sci 2004;117:2805 – 12.
32. Mizushima N. Methods for monitoring autophagy. Int J Biochem Cell Biol 2004;36:2491 – 502.
33. Blommaart EF, Krause U, Schellens JP, Vrelling-Sindelarova H, Meijer AJ. The phosphatidylinositol 3-kinase inhibitors wortmannin and LY294002 inhibit autophagy in isolated rat hepatocytes. Eur J Biochem 1997;243:240 – 6.
34. Walker EH, Pacold ME, Perisic O, et al. Structural determinants of phosphoinositide 3-kinase inhibition by wortmannin, LY294002, quercetin, myricetin, and staurosporine. Mol Cell 2000;6:909 – 19.
35. Onodera J, Ohsumi Y. Autophagy is required for maintenance of amino acid levels and proteins synthesis under nitrogen starvation. J Biol Chem 2005;280:31582 – 6.
36. Komatsu M, Waguri S, Ueno T, et al. Impairment of starvation-induced and constitutive auophagy in Atg7-deficient mice. J Cell Biol 2005;169:425 – 34.
37. Levine B, Yuan J. Autophagy in cell death: an innocent convict? J Clin Invest 2005;115:2679 – 88.

38. Eskelinen EL. Doctor Jekyll and Mister Hyde: autophagy can promote both cell survival and cell death. Cell Death Differ 2005;12 Suppl 2: 1468 – 72.

39. Tibes R, Lu Y, Siwak DR, et al. Identification of selective inhibition of phospho-S6 ribosomal protein in XK469 sensitive leukemia cell lines using functional proteomic analysis. Abstr 3279, 96th meeting Am Assoc Cancer Res; 2005.

40. Klionsky DJ, Meijer AJ, Codogno P, Neufeld TP, Scott RC. Autophagy and p70S6 kinase. Autophagy 2005;1:59 – 61.

41. Blommaart EF, Luiken JJ, Blommaart PJ, van Woerkom GM, Meijer AJ. Phosphorylation of ribosomal protein S6 is inhibitory for autophagy in isolated rat hepatocytes. J Biol Chem 1995;270:2320 – 6.

42. Takeuchi H, Kondo Y, Fujiwara K, et al. Synergistic augmentation of rapamycin-induced autophagy in malignant glioma cells by phosphatidylinositol 3-kinase/protein kinase B inhibitors. Cancer Res 2005;65: 3336 – 46.

43. Lemasters JJ, Nieminen AL, Qian T, et al. The mitochondrial permeability transition in cell death: a common mechanism in necrosis, apoptotsis and autophagy. Biochim Biophys Acta 1998;1366:177 – 96.

44. Lemasters JJ. Selective mitochondrial autophagy, or mitophagy, as a targeted defense against oxidative stress, mitochondrial dysfunction, and aging. Rejuvenation Res 2005;8:3 – 5.

45. Munz C, Autophagy and antigen presentation. Cell Microbiol 2006;8: 891 – 8.

Molecular Cancer Therapeutics

The role of autophagy in the death of L1210 leukemia cells initiated by the new antitumor agents, XK469 and SH80

David Kessel, John J. Reiners, Jr., Stuart T. Hazeldine, et al.

Mol Cancer Ther 2007;6:370-379.